POLITECNICO DI TORINO
Repository ISTITUZIONALE

EE-BESD: Molecular FET Modeling for Efficient and Effective Nanocomputing Design

(Article begins on next page)

31 July 2024

EE-BESD: Molecular FET Modeling for Efficient and Effective Nanocomputing Design

A. Zahir · A. Pulimeno · D. Demarchi · M. Ruo Roch · G. Masera ·
M. Graziano · G. Piccinini

-

Abstract Molecular transistor is a good candidate as substitute of CMOS device due to small size, expected good performance and suitability to be included in high density-circuits.

To date a lot of effort has been carried out to understand the conduction properties in molecular devices. However, minor effort has been devoted to reduce their computational complexity to obtain a compact molecular model.

First-principle based methods frequently used are highly computational demanding for a single device, thus they are not suitable for complex circuit design.

In this paper we present an accurate and at the same time computationally efficient method (named Efficient and Effective model based on Broadening level, Evaluation of peaks, Scf and Discrete levels, EE-BESD) to calculate the electron transport characteristics of molecular transistors in presence of applied bias and gate voltages.

The results obtained show a remarkable improvement in terms of computational time with respect to existing approaches, while maintaining a very good accuracy. Finally, the EE-BESD model has been embedded in a circuit level simulator in order to show its functionalities and, particularly, its computational cost. This is shown to be affordable even for circuits based on a high number of devices.

A.Zahir, A.Pulimeno, D.Demarchi, M.Ruo Roch, G. Masera, G. Piccinini
Electronics and Telecommunication Department, Politecnico di Torino, Italy E-mail: azzurra.pulimeno@polito.it, gianluca.piccinini@polito.it

M.Graziano
Electronics and Telecommunication Department, Politecnico di Torino, Italy and London Centre for Nanotechnology, UCL Physics and Astronomy Department m.graziano@ucl.ac.uk

1 Introduction

Molecular device features [1–4] pave the way for highly dense and low power future computing applications [5–8]. On one hand, the availability of hierarchy of interconnect and device models of varying accuracies for silicon technology allows circuit designer to efficiently simulate complex circuits [9–13]. On the other hand, in molecular electronics the detailed physical and chemical description of transport is computationally complex and it can not be tackled when the number of devices combined in interconnected functional structures increases. As a consequence, in order to exploit molecular electronics potentials in the design of complex high performance systems, efficient simulation methodologies are needed.

In the literature, the Huckel theory [14] first, Density Function Theory (DFT) [15,16] later and more recently Non Equilibrium Green Function (NEGF) [17] have been used to study and describe the electron transport in molecular systems. In particular, an effective solution to reproduce the $I - V$ characteristics of experimental molecular systems is a combination of DFT and NEGF methods [18]. The main advantage of this approach is to rigorously treat the open boundary condition and the influence of applied bias voltage. However, to achieve accurate $I - V$ characteristics for each applied bias, transmission spectrum is normally recalculated by DFT-NEGF method using self-consist field (SCF) loop. This method in the presence of charge effect in SCF regime demands high computational re-
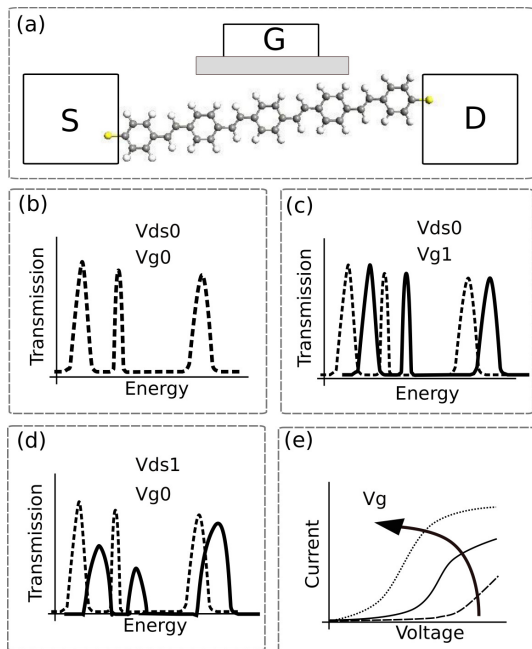
Fig. 1 (a) Schematic diagram of molecular FET. (b) Transmission spectrum of Oligo Phenylene Vinylene (OPV) molecular FET when a gate voltage (V_{g0}) and a drain-source voltage (V_{ds0}) are applied. (c) A variation of the drain-source voltage from V_{ds0} (dotted line) to V_{ds1} (solid line) causes a reshaping of the spectrum peaks. (d) The transmission spectrum at V_{g1} (solid line) and V_{g0} (dotted line) is presented to show the effect of the gate voltage. (e) The $I - V$ characteristics of OPV molecular FET are reported for different gate voltages V_g.

quirements. This approach is not suitable for describing and simulating molecular nanosystems, where millions of devices are supposed to be interconnected in order to implement complex realistic functions as in silicon technology.

The purpose of the present work is to propose a *model that can accurately estimate non equilibrium electron transport characteristics of molecular FET (molFET) with very low computational complexity*. The proposed model (named EE-BESD as will be discussed in section 3) has been developed on the basis of the molecular system shown in Figure 1(a). The molecular transistor can be obtained anchoring a molecule between two metallic electrodes (S,D) with an electric field applied perpendicularly to the channel using a third gate electrode (G) to exploit the field effect. The transmission spectrum of the molecular electronic system is dependent on the applied external voltages, i.e. source-drain voltage V_{ds} and gate voltage V_g. An abstract example of transmission spectrum of the above mentioned system is in figure 1(b). We exploit two main properties that we observed by analyzing physical level simulations. A V_g variation (from V_{g0} to V_{g1}) causes a rigid shift of the transmission spectrum peaks as sketched in Figure 1(c). Similarly, a

variation of the applied V_{ds} (from V_{ds0} to V_{ds1}) causes a reshaping of the spectrum peaks that change both shape and energy value for the peak (an example in Figure 1(d)). In both cases, the changes have trends that can be analyzed and used in the modeling phase. Consequently the $I - V$ characteristic (Figure 1(e)) can be obtained by combining the above mentioned analyses on how the transmission spectrum evolve. Exploiting the observations and assumptions in the modification of transmission spectrum result in significant reduction of computational overhead. This reduces the simulation time while the accuracy of the system remains not far from atomistic level simulations. Overall, our contribution is then twofold: 1) To reduce the state of the art in terms of computational time compared to first principle method based atomistic simulations; 2) to maintain a near to optimal accuracy, improved with respect to other modeling approaches [18]. The proposed model EE-BESD presented in our study can be valuable in guiding and analyzing wide variety of complex molecular electronic applications.

The rest of the paper is arranged as follows. The related work is explained in section 2. Detailed methodology of the model is discussed in section 3. Section 4 covers the results and validation of the model. And section 5 concludes the paper.

2 Related Works

Since the idea of Aviram and Ratnes [19] to use molecular device as an active element, the field of molecular electronics has gained a lot of interest.

On experimental side, interesting transport properties such as conductance, tunneling and resistance of molecular bridge between two electrodes have been explored and discussed [20–26]. Recently, interest has been received by three terminal devices and many gated molecular devices [27–31] have been experimentally demonstrated. Lee et al [27] observed a weak gate effect for 1,3 Benzeneditiol (BDT) molecule. Song et al. [28] demonstrated that the electrostatic modulation of orbital of 1,4 benzenedithiol (BDT) and octaneditiole (ODT) systems can be effectively controlled by the gate voltage.

On theoretical side, a lot of studies based on first principle or semi-empirical based methods have been done in order to understand, control and explain charge transport of two terminal [32–38] and three terminal [39–42] molecular devices.

DFT-NEGF is used to qualitatively reproduce the $I-V$ characteristics of experimental molecular systems. Using self-consistent first principle calculation, [40] and [39] explain the dependency of transistor efficiency on

geometrical shape of gate and contact coupling between molecule and metal.

In [43], the behavior of three terminal electron transport has been examined considering a single benzene molecule attached to three terminals. The molecular system is described by simple tight binding Hamiltonian. The numerical calculation based on Greens function approach is used to illustrate the detailed behavior of multi terminal conductance, rectification probability and I-V characteristics. The charge transport variation of OPV molecular system with gate bias is characterized in [41] using NEGF in combination with Extended Huckel Theory (ETH).

The transport behavior of OPV based molecular device with a back gate is analyzed, considering output current dependency on gate voltage. Other interesting transport behavior like negative differential resistance and the inversion in the relation of gate conductance at some negative gate bias are also observed. However, the first principle method demands high computational requirements.

Different approximation methods have been discussed in theory for computational speed up. An analytical model for two terminal device with low computational demands is presented in [35] by combining mesoscopic transport and first-principle method. In the method, DFT is used to calculate energy levels and level dependence on applied voltage. The extracted parameters are then translated into mesoscopic transport model to calculate $I-V$ characteristics. In another study, to speed up DFT calculation, a non linear multigrid method [33] is used to find the $I-V$ characteristics of two terminal metal-molecule-metal system. However, the transmission spectrum is considered independent of bias voltage.

Recently, authors in [44] present a technique for modeling molecular devices using circuit elements and employed the models to simulate molecular devices in SPICE. The circuit model is NMOS with typical parameter values and different V_{th} depending on the type of modeled molecules, atoms or insulating alkane chains. Two parallel NFET are used to account the mutual interaction of two neighboring atoms in a chain. For three terminal device, the electrostatic coupling of the gate to molecule is introduced by coupling parameter.

In our proposed model level shifts with applied voltage is calculated using self-consistent method, thus avoiding DFT calculation for level dependence. In this paper we propose a method for three terminal devices which includes the dependence of transmission spectrum on applied bias voltage with low computational overheads.
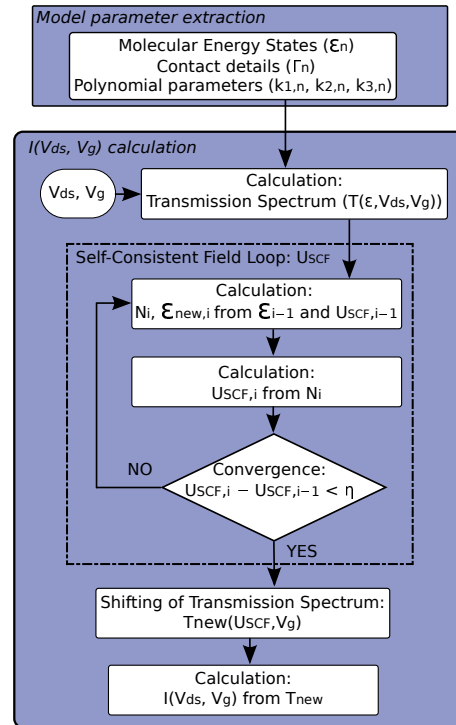

Fig. 2 Algorithm for calculating the current with the proposed model EE-BESD: the preliminary step is the extraction of some parameters from atomistic simulations, that will be provided as inputs to the current calculation flow. This flow is mainly divided in three phases: the calculation of the transmission spectrum ($T(\mathcal{E}, V_{ds})$), the SCF loop and, finally, the calculation of current ($I(V_{ds}, V_g)$).

3 Methodology

Figure 2 shows the algorithm flow of our proposed model for the calculation of current in molecular transistor. Hereinafter we will refer to it as EE-BESD; the acronym derives from the types of approximations and methods used and will be clear after a thorough explanation at the end of this section.

The proposed algorithm requires the preliminary extraction of some parameters for a specific molecule suitable for MolFET technology obtained by atomistic simulations. In this paper we use as reference software Atomistix ToolKit (ATK) [45][46]. As depicted in the *Model parameters extraction* box (Figure 2, top rectangle), these parameters are: the molecular energy states ($\mathcal{E}_n$, where n is a reference to the n_{th} orbital), the coupling strength (Γ_n) of the two metal-molecule contacts and the polynomial coefficients ($k_{1,n}, k_{2,n}, k_{3,n}$), obtained and used as discussed in Section 3(A). Afterwards, the extracted parameters become inputs for the $I(V_{ds}, V_g)$ *calculation* phase (Figure 2, main blue rectangle) and they are used to find voltage dependent transmission spectra ($T(\mathcal{E}, V_{ds}, V_g)$), as discussed in Sec. 3(B). Then, the self-consistent-field (SCF) loop

is involved in the algorithm (inner dash-dotted rectangle in the figure) as further on analyzed in Sec. 3(C). The necessity of this loops derives from the fact that the electrons, when moving from one electrode to the other, influence the potential energy of the metal-molecule-metal system, leading to a shift of the transmission spectrum. This loop, thus, with this successive approximation approach, estimates the correct potential energy U_{SCF} with an approximation level that can be decided by the user. In addition, the algorithm computes the effect of the gate voltage (V_g) on the transmission spectrum, as described in Section 3(E). Thus, finally, the current $I(V_{ds}, V_g)$ is calculated as function of the bias conditions and the obtained transmission spectrum (Sec. 3(D)).

Results are discussed in section 4. The algorithm is tested first on an OPV molecule. The OPV current as function of the bias voltage is obtained and used as a fundamental curve to compare the effects of the assumptions and approximation done by the proposed EE-BESD method with the effects due to different approximation methods adopted in other works. In all the cases the result of the first principle based atomistic simulation is used as reference point. The EE-BESD method is then used to compare the results for a few other types of molecules, and the error in the I-V curve approximation is measured with respect to the values obtained using the commercial atomistic simulator. Finally, the efficiency of the algorithm is estimated when used in a circuit level simulator based on VHDL-AMS language and when a high number of devices is included in the simulation.

The rest of this section is dedicated to the detailed explanation of the algorithm.

A. Model parameters extraction

Transport properties of metal-molecule-metal are usually dominated by the molecular energy levels that are close to the Fermi energy level. These levels are known as Highest Occupied Molecular Orbitals (HOMOs) or Lowest Unoccupied Molecular Orbitals (LUMOs). In order to properly estimate these energy levels by atomistic simulations we used a simulation environment based on ATK. The analyzed molecular system, as shown in Figure 1, involves an optimized molecule placed between two gold Au(111) electrodes (built as 4x4 atoms), with an optimum distance between molecule and electrodes [34]. This distance depends on the type of molecule and, for example, for the OPV molecule it is 1.71 AA as reported in [34]. Regarding the simulation frame, electrode layers from either side (left L and right R) are extended into the device region, in order to take into account the effect of metal-molecule interaction [34]. For DFT exchange correlation we use local density approx-

Table 1 Parameters for transmission spectrum calculation of OPV molecule.

n	Orbital	$\mathcal{E}_n$ (eV)	Γ_{L_n/R_n} (eV)	Γ_n (eV)	k_1	k_2	k_3
1	HOMO	-1.95	0.010	0.02	0.13	-0.53	0.7
2	LUMO	0.15	0.025	0.50	0.05	0.32	1.0
3	LUMO+1	0.60	0.050	0.10	-0.02	0.40	0.9
4	LUMO+2	1.20	0.050	0.10	-0.02	0.40	0.9

imation (LDA) with unpolarized spin and 100 points in C direction. Transmission spectrum and details of energy level of the molecular system are calculated using Kyrlov [47] self-energy calculator.

Data obtained by these simulations are used to set important parameters adopted in the proposed algorithm to define the transmission spectrum for different bias voltages. Oligo Phenylene Vinylene (OPV) molecule is considered here as an example. Table 1 shows four molecular orbitals $\mathcal{E}_n$ ($\mathcal{E}_1$: HOMO, $\mathcal{E}_2$: LUMO, $\mathcal{E}_3$: LUMO+1 and $\mathcal{E}_4$: LUMO+2) near to Fermi level and their coupling strengths for L and R Γ_{L_n/R_n}. The $I - V$ characteristics mainly depend on the contribution of these four molecular orbitals for the applied voltage range (in this work defined as $V_{ds} = -3 \div +3V$, as usually suggested in literature for MolFET devices). We assumed that right R and left L contacts are symmetrical, thus their coupling strengths Γ_R and Γ_L are the same. Γ is the width of the broadened energy level [36–38]. Coupling strength of the molecular system ($\Gamma_{L/R}$) is guessed nearly half of the width of the corresponding transmission peak obtained by atomistic simulations [36–38]. k_1, k_2 and k_3 are constant coefficients used in the model to define the evolution of the transmission peaks according to the applied voltage by means of a second-order polynomial (see Sec. 3(B)). These constants are estimated once and for all by curve fitting, using as a reference a limited set of transmission spectra curves related to a few specific V_{DS}.

B. Calculation of transmission spectrum

For each $\mathcal{E}_n$ and given the extracted parameters in Table 1, the transmission spectrum $T(\mathcal{E} - \mathcal{E}_n)$ of molecular orbitals is obtained by equation 1 as suggested in [36,38]:

$$T(\mathcal{E}) = \frac{\Gamma_{L_n} \Gamma_{R_n}}{(\mathcal{E} - \mathcal{E}_n)^2 + (\Gamma_n/2)^2}. \tag{1}$$

Fig. 3(a-d) shows the transmission spectra of each single molecular orbital obtained using equation 1 at equilibrium. The complete transmission spectrum could be computed as a superposition of the functions obtained by equation 1 for each molecular orbitals. For the OPV molecule, the complete transmission spectrum

obtained by model EE-BESD is shown in Figure 3(e) (solid line). The same transmission spectrum obtained by atomistic simulation (dashed line) is shown as well for sake of comparison.

The phenomenon of change in transport properties after applying voltages can be viewed in terms of evolution of transmission spectrum. The applied voltage affects the transmission spectrum in two ways: 1) changing the position of molecular orbitals relative to the Fermi level of electrode and 2) broadening of molecular orbitals. Moreover, also a variation of V_G changes the energy levels with respect to the Fermi value. This influence is analyzed in section 3.E, while herein and in the following subsection the first two effects are discussed.

The applied bias voltages affect the area of the transmission spectrum of the molecular system: the change of the transmission peaks with applied bias in EE-BESD is approximated with a quadratic polynomial (β_n, defined by equation 3). In our model the choice of this kind of polynomial is a trade-off between accuracy and computational efficiency. In this version of the algorithm we privileged the estimation in terms of peaks position and peak area values, neglecting the change of the shape of the peaks with V_{ds}. This choice derives from observing that even with ATK simulations the broadening has a very limited change in terms of shape if compared to the peak area and position variations. These are then the approximations done when estimating the broadening effect mentioned throughout the paper. The bias dependent transmission spectrum is obtained by

$$T(\mathcal{E}, V_{ds}) = \sum_n \beta_n(V_{ds}) T(\mathcal{E} - \mathcal{E}_n), \qquad (2)$$

where β_n is used to include bias induced changes of transmission spectrum in Eq. 2. The factor β_n is dependent on the bias voltage as second degree polynomial as in the following

$$\beta_n = k_1 |V_{ds}^2| + k_2 |V_{ds}| + k_3, \qquad (3)$$

where k_1, k_2 and k_3 are constants whose values are estimated by using curve fitting (see Sec. 3(A)). For OPV molecule their values are given in Table 1.

C. Self-Consistent-Field loop (SCF).

As mentioned above one of the effect of the bias voltage is a shifting of the transmission spectrum. In our model, the relative position of peaks in energy (e.g. the position of one peak with respect to the other) is not affected by bias voltages. As a consequence, in EE-BESD the complete transmission spectrum is always rigidly shifted in energy, and the shift depends on V_{ds}, V_g and
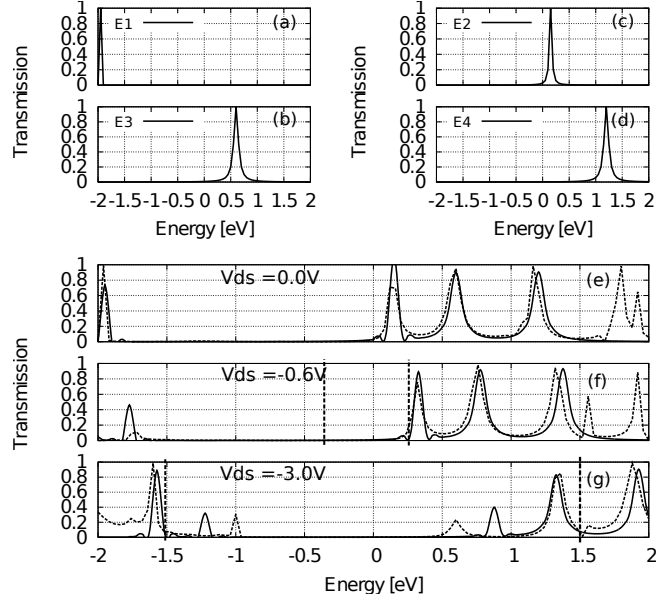

Fig. 3 Transmission spectrum as a function of energy for OPV molecule. (a)-(d) Transmission spectrum of individual molecular orbitals ($\mathcal{E}_n$). (e-g) Transmission spectrum of the molecular device obtained by proposed methodology for different bias voltages. For comparison, transmission spectrum obtained by Atomistix simulation [45,46] is also shown (dashed lines). The vertical dotted lines highlight the bias window due to V_{ds}.

on the charge hosted by molecular levels (charging effect). As suggested in [35] for low applied voltages the molecular levels show a linear shift.

Charging effect produces a shift of transmission spectrum and it is accounted for in the self-consistent field (SCF, [36,38]) loop in the algorithm (the inner dash-dotted rectangle in the algorithm flow). The shifting depends on the self-consistent field energy (U_{SCF}) related to the charge hosted in the molecular orbitals. At each step of the loop, the energies of molecular orbitals $\mathcal{E}_{n,i}$ are re-calculated by adding self-consistent field energy U_{SCF} as in the following equation

$$\mathcal{E}_{n,i} = \mathcal{E}_{n,i-1} + U_{SCF}. \qquad (4)$$

The self-consistent field energy is computed from electron population using

$$U_{SCF} = U_0(N - N_0), \qquad (5)$$

where U_0 is charging energy for a single electron and is equal to 1eV. N_0 is the total number of electrons hosted by the energy levels of the molecular system at the equilibrium and is equals to $N_0 = 2f_0$, where f_0 is the Fermi function at the equilibrium ($V_{ds} = 0V$ and $V_g = 0V$). N is the sum of the electrons hosted by all
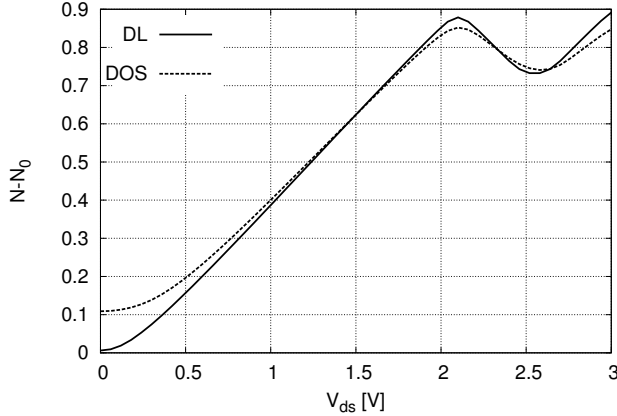
Fig. 4 Change in number of electrons $(N - N_0)$ obtained by discrete level (DL) and energy-level broadening (DOS).

Fig. 5 Comparison of $I-V$ characteristics for OPV molecule using different methods. Atomistic simulation (solid line) is considered as a reference. The proposed model EE-BESD $(BL + EP + SCF_{DL}$, dashed line) considers evaluation of transmission spectrum peaks with applied bias, while other two methods ($BL + SCF_{DL}$ and $BL + SCF_{DOS}$) ignore evaluation of transmission peak. BL: energy-level broadening, EP: evaluation of transmission spectrum peak, SCF_{DOS}: self-consistent loop using energy-level broadening and SCF_{DL}: self-consistent loop using discrete levels.

the energy levels involved in the conduction and it is expressed by equation (6) as suggested in [36–38]:

$$N = 2 \sum_n \frac{\Gamma_{L_n} f_{L_n}(\mathcal{E}_{n,i}) + \Gamma_{R_n} f_{R_n}(\mathcal{E}_{n,i})}{\Gamma_{L_n} + \Gamma_{R_n}}, \quad (6)$$

where f_{L_n} and f_{R_n} are the Fermi-Dirac functions of left and right electrodes, respectively. Equations (6) and (5) are calculated iteratively until the convergence is achieved. In particular, defined the desired accuracy η, the iterations end when:

$$U_{SCF,i} - U_{SCF,i-1} < \eta. \quad (7)$$

The value N obtained as mentioned above is related to the discrete energy levels DL of the spectrum. However, if we consider the broadening of the energy levels as well, the number of electrons N should take also into account, in theory, the occupancy of each energy level given by the Density Of States (DOS). This is done for example in the Atomistix ToolKit (ATK) [45] used here as a reference. For sake of comparison, in figure 4 the results of $N - N_0$ are reported for different V_{ds} in both cases of discrete levels (proposed EE-BESD model) and broadening (DOS, obtained using ATK). The approximation introduced considering the discrete levels is good and reasonable for a wide range of bias voltages. Moreover, the discrete level approximation used in the *Self-Consistent-Loop* gives a remarkable advantage in terms of computational efficiency if compared to the effort spent by ATK in including the effect of broadening. In the same time it still provides a good estimation of the molecular orbital shift. For the sake of comparison, transmission spectrum obtained by fully self-consistent DFT-NEGF using ATK (broadening, dash lines) and the proposed model (solid line) for different voltages are shown in Fig. 3(e-g). Hereinafter, the DFT-NEGF
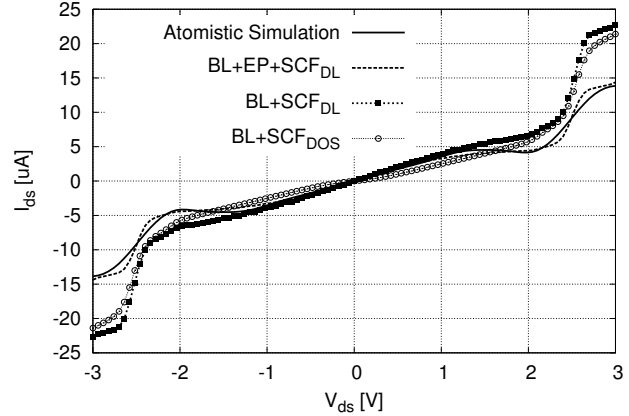
calculation obtained by ATK will be referred as atomistic simulation.

D. Calculation of Current

Finally, referring to the last step of the flow diagram, the new current I is calculated using the modified transmission spectrum and the Landauer [36] formula in equation 8:

$$I(V_{ds}) = \frac{2q}{h} \int_{-\infty}^{\infty} T(\mathcal{E}, V_{ds})(f_L(\mu_L) - f_R(\mu_R))d\mathcal{E}, \quad (8)$$

where f_L and f_R are again the Fermi-Dirac functions of left and right electrodes, respectively, while μ_L and μ_R are the chemical potential of the same electrodes.

It is at this point interesting to analyze on the $I - V$ characteristic the impact of different types of approximation. Fig. 5 shows this comparison for an OPV molecular device. In the figure the current obtained by atomistic simulation (solid line) [45, 48] is used as a reference. The possible approximations that can be considered in the calculation of current are: 1) energy-level broadening (BL) with the approximations as defined in section 3.B, 2) evaluation of peaks of transmission spectrum with applied voltages (EP), 3) self-consistent field loop using energy-level broadening (SCF_{DOS}) and 4) self-consistent field loop using discrete levels (SCF_{DL}). The proposed method EE-BESD involves approximations 1, 2 and 4 $BL + EP + SCF_{DL}$ is used in the figure
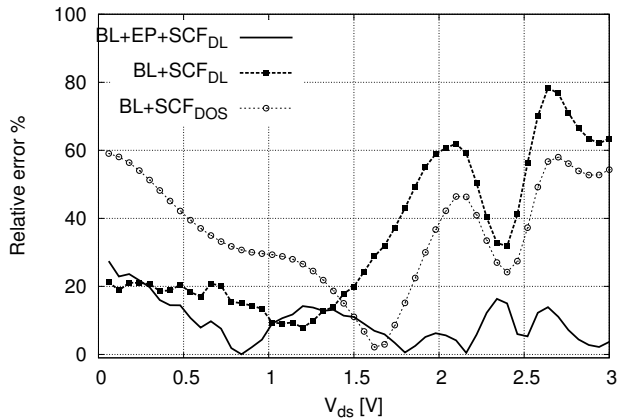
Fig. 6 Comparison of the relative error of the $I - V$ characteristics for OPV molecule using different methods with respect to atomistic simulations. The proposed model EE-BESD ($BL + EP + SCF_{DL}$, solid line) estimates the current better than the other two approximations ($BL + SCF_{DL}$ and $BL + SCF_{DOS}$, dashed lines).

to identify the obtained current (and from this mixture the first letters are used in the proposed model acronym for sake of simplicity: BL, EP, SCF, DL)). Figure 5 also includes the results obtained with two other sets of approximations: 1 and 4 ($BL + SCF_{DL}$); 1 and 3 ($BL + SCF_{DOS}$), as proposed in [36,38]. The proposed model EE-BESD is clearly a good compromise between accuracy and computational effort, since the results shown in Figure 5 compares well with the results of atomistic simulation. The other two methods overestimate currents at high voltages. Moreover, in the case of $BL + SCF_{DOS}$ the SCF_{DOS} is quite expensive, as it happens in ATK. The results section gives details on the computational advantages.

Figure 6 shows the relative error of the current estimated by the three sets of approximations ($BL + EP + SCF_{DL}$, $BL + SCF_{DL}$ and $BL + SCF_{DOS}$) with respect to the results obtained with atomistic simulations. The proposed model EE-BESD is clearly the most accurate, since the relative error is the smallest compared to the other two approximation sets. For very low bias voltages, the relative error of EE-BESD is slightly greater than 20% and this is due to the very small values of the current when the transistor is off. At high voltage, when the molecule is in conduction mode (the transistor is on) the relative error is always under 20%, while the other two approximations overestimate the current for about 60% or even 80%. The accuracy of the model is important to predict the single device performance in terms of speed and power consumption, as well as the dynamic behavior of the device. In addition, an accurate model could be useful for the transistor sizing

in a gate and for the functional analysis of a circuit with cascode transistors. From an application perspective the EE-BESD error can be considered acceptable, since the impact on circuits behavior is expected to be very limited. The reference is in this case ATK, which is considered to have a solid theory and that is widely used as a reference point in the scientific scenario. More reliable comparisons could be done with measurements. However, in the case of nanometer sizes molecular devices the technology is rich of challenges not only in terms of fabrication but also in terms of measurements, as for example revised in [49].

E. Gate voltage effect

In three terminal device, the gate voltage also shifts the molecular energy levels relative to E_f. For each energy level, the effect of the shifting can be accounted as in Eq.(9)

$$\mathcal{E}'_n = \mathcal{E}_n - q|\alpha|V_g, \tag{9}$$

where α is the gate coupling factor. This factor can be measured from Fowler-Nordheim plot of $I - V$ characteristic of molecular transistor [28]. The obtained $\mathcal{E}'_n$ are then used in the self-consistent field loop as described in Sec.3D.

4 Results

In this section, we illustrate the results of employing our modeling methodology to different molecular systems: Oligo Phenylene Ethynylene (OPE), Oligo Phenylene Vinylene (OPV) and Thiophene molecules with different lengths varying from three rings (3TT) to five rings (5TT). All the molecules have sulfur linker on both terminals. In order to have a reference point for verification, fully self-consistent DFT-NEGF method using atomistic simulation [45,48] is used for above cases. Then, the behavior of molecular transistor for different gate voltages is compared with the state of the art literature. The analysis of the gate voltage on the transmission spectrum of molecular transistor is then presented. Finally, results on the application of the model to a circuit level description based on VHDL-AMS language are presented and discussed.

1) Transmission spectrum and IV Characteristics.

Equation (8) integrates the spectrum modulated by the difference of the Fermi function between source and drain to compute the current in the bias window. Therefore, an interesting and meaningful analysis consists
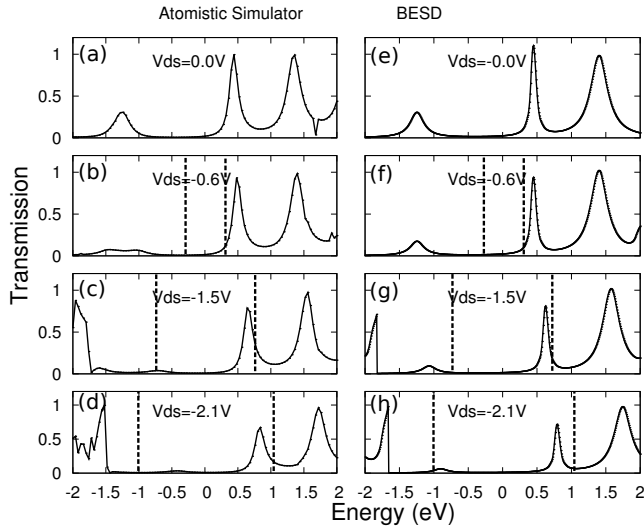
Fig. 7 Transmission spectrum as a function of energy of OPV molecule at different bias voltage and $V_g = 0V$. Vertical dotted lines represent the bias window over which current is calculated. (a)-(d) are obtained using atomistic simulations [45, 48] and (e)-(h) are obtained using the proposed model EE-BESD $(BL + EP + SCF_{DL})$. The Fermi level (E_f) is the average value of the chemical potential of the left and right electrodes.

Fig. 9 Comparison of the area of the integral of the transmission spectrum covered by electrode chemical potential as a function of bias voltage of different molecules at zero gate voltage (a) OPV, (b) OPE, (c) 3TT, (d) 4TT and (e) 5TT. Dashed lines represents the proposed model results and the dots are related to atomistic simulation [45, 48] results.

in comparing the transmission spectra at different applied voltages obtained by EE-BESD to those reckoned through the atomistic simulations. Figure 7 shows the transmission spectra of the OPE molecule obtained by the two methods for three conditions of bias voltage: $V_{ds} = -0.6V$ ($V_d = -0.3V$ and $V_s = +0.3V$), $V_{ds} = -1.5V$ ($V_d = -0.75V$ and $V_s = +0.75V$), $V_{ds} = -2.1$ ($V_d = -1.05V$ and $V_s = +1.05V$). For all these cases, in figure 7(b-d) and (f-h) the bias window is delimited by the two vertical dashed lines. In the current I calculation, the main contribution is due to the peaks that are included in the bias window. Figure 7(a) corresponds to the transmission spectrum at equilibrium. Considering the transmission spectra obtained using atomistic simulations (a-d), at small bias voltage in absolute value ($V_{ds} < -0.6V$), LUMO orbital does not contribute to the conduction. Increasing (in absolute value) the bias voltage, the conduction is dominated by LUMO peak, since the HOMO orbital is further reduced in the shape, as shown in figure 7(b) and (c). On further increase of the bias voltage ($V_{ds} = -2.1V$), the LUMO peak of the transmission spectrum is completely inside the bias window. Figures 7(e-h) show the transmission spectrum obtained by model EE-BESD for the same bias conditions. These results clearly pinpoint how the shift of the transmission spectrum, as well as the evolution of peaks, are well described by EE-BESD.
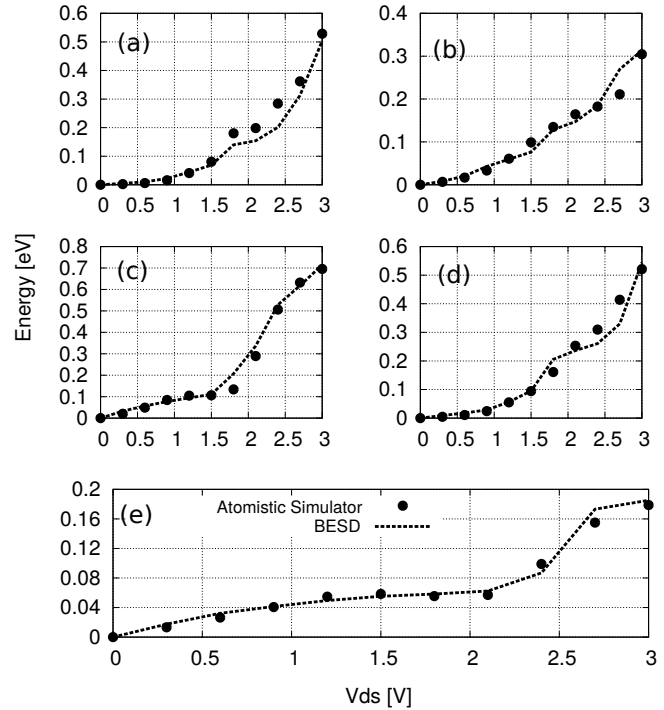
In order to verify the proposed model, the $I - V$ characteristics of different molecular systems are compared to atomistic simulations, as shown in Fig. 8. For all the molecules the applied voltage range is symmetrical and sweeps from $-3V$ to $3V$, with a step of $0.03V$ for the proposed model and a step of $0.3V$ for atomistic simulations. In the latter, the voltage step is much higher than in the proposed model to limit the atomistic simulation time (see Table 2 in *Computational analysis* subsection for details). For all the curves, we computed the absolute error between the proposed model current and the current computed by ATK. As depicted in figure 8, the absolute error is almost negligible when the current values are low (low applied voltages), and it is very small when the molecules start conducting. This confirms the accuracy of the proposed EE-BESD model in computing the quantum transport in molecules.

The $I - V$ characteristics of a molecular system are determined mainly by the area of the integral of the transmission spectrum covered by the electrode chemical potential. Thus for further verification, we compare the integral area of different molecular systems, shown in Fig. 9, obtained by both atomistic simulation and proposed model and they are in very good agreement.
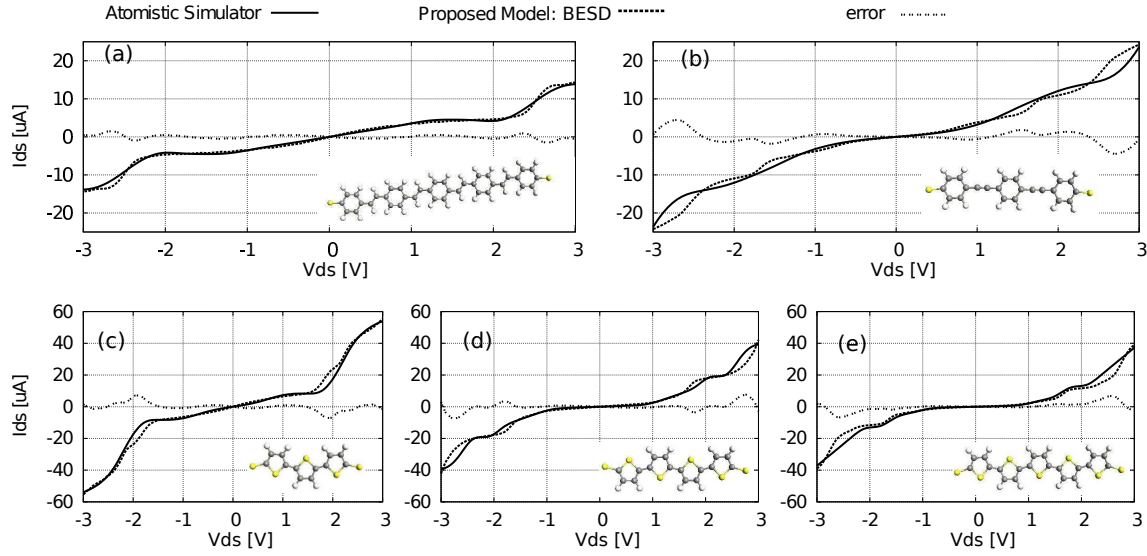
Fig. 8 Comparison of $I - V$ characteristics of different molecules at zero gate voltage (a) OPV, (b) OPE, (c) 3TT, (d) 4TT and (e) 5TT. In all the figures, results obtained by proposed model EE-BESD (BL+EP+SCF-DL, dashed lines) are compared to DFT-NEGF method results (solid lines) obtained by atomistic simulation [45, 48].
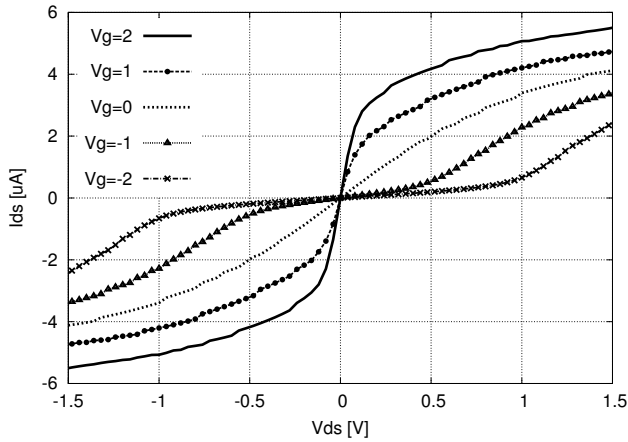

Fig. 10 $I - V$ characteristics of OPV molecule obtained by the proposed model EE-BESD (BL+EP+SCF-DL). Gate voltage varies from $-2V$ to $2V$ with $1V$ step. The current is maximum at $V_g = 2V$ and decreases as V_g decreases.

2) Effect of the gate voltage on electrical conduction of molecular transistor

A detailed analysis on the effect of gate voltages on the transmission spectrum is performed to show that the proposed model can be used in circuit level simulations for molecular transistor [39, 41, 42].

From experimental [28] and theoretical [39] studies, the gate efficiency factor $|\alpha|$ defined in equation (9) varies from 0.22 to 0.32. In this study we take $|\alpha| = 0.25$. As OPV molecular transistor is LUMO type, positive gate voltages lead to an increase of the electron

population inside the bias window and thus enhance the current. Similarly, negative gate voltages reduce the number of electrons involved in conduction, thus reducing the current.

This behavior can be explained evaluating the transmission spectrum. Figure 11 depicts calculated transmission spectrum of OPV system for different gate voltages. In Fig. 11 OPV is LUMO dominating, thus a negative gate voltage shifts LUMOs level towards high energies away from E_f, while HOMOs are pushed towards E_f. In the same manner, a positive gate voltages increases the conduction by pushing LUMOs towards Fermi level. These shifts in HOMOs and LUMOs levels due to gate voltages are translated into shift of the peak in the transmission spectrum, which results in an increase in the current as shown in figure 10 for the OPV molecule.

The impact of the gate voltage on the transconductance behavior can be found by simulating the conductance as function of gate voltage at bias $V_{ds} = 0.5V$ as shown in Fig. 12 for the OPV molecule (dI_{ds}/dV_g). The conductance increases with the gate voltage varying from $-4V$ to $3V$. For gate voltage values below $-4V$ the transconductance changes the sign. In order to highlight this phenomenon, the derivative of the current with respect to the gate voltage is reported in figure 12 (dI_{ds}/dV_g, solid lines) This behavior is also observed in [41, 42]. The origin of this phenomenon is the shift of the molecular level with respect to E_f. The gate voltages below $-4V$ shift the HOMO orbital level very near to the the E_f. At this stage, the conduction type
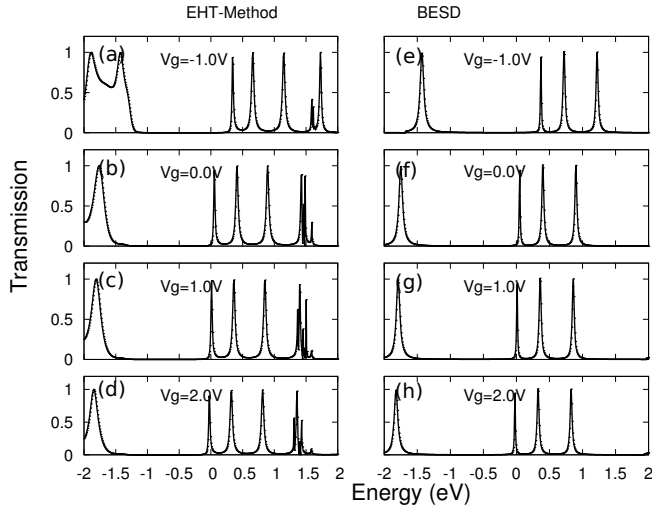
Fig. 11 Transmission spectrum as a function of energy of OPV molecule at different gate voltages (V_g). (a)-(d) are obtained using atomistic simulations [45] and (e)-(h) are obtained using the proposed model EE-BESD.
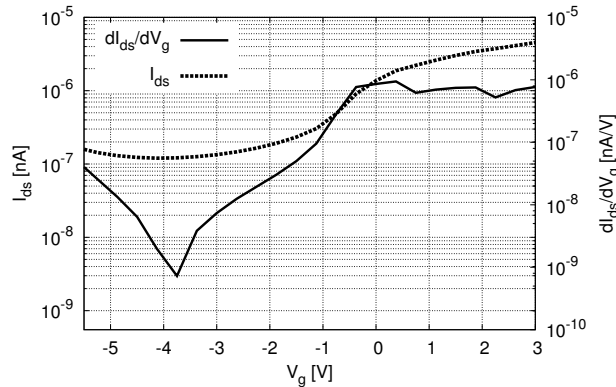

Fig. 12 Current as a function of gate voltage (I_{ds}, dashed line) at $V_{ds} = 0.5V$ obtained for the OPV molecule by proposed model. The solid line represents the derivative of the current with respect to the gate voltage (dI_{ds}/dV_g)

is changed from LUMO to HOMO. As a consequence lowering the gate voltage will increase current.

Another important factor is the non-linear behavior of the gate control on transmission spectrum as studied in [39,40] for different molecules. The shift of transmission spectrum is strongly dependent on the applied gate voltage. Figure 11 shows the effect of the gate control on transmission spectrum: when the LUMO peak is inside the bias window (Fig. 11(f),(g) and (h)), the feedback from self-consistent field makes the effect of the gate voltage weaker. This results in the reduction of the gate control on the transmission spectrum.

3) Computational analysis

Table 2 shows the timing analysis of self-consistent field loop (SCF), transmission spectrum ($T(\mathcal{E})$) and current (I) calculations of the proposed method and the other methods studied in this work, as well as for all the molecules under analysis. In all the cases, we run our simulations on a machine having 16 Intel Xeon 2.40 GHz processors and 16 GB RAM. For methods BL+SCF-DL, BL+EP+SCF-DL (proposed EE-BESD) and BL+SCF-DOS, simulations are run for 2000 times and the average time is considered. For these three methods the MatLab profiler was used to get the timing information, while for the atomistic simulations all the information were provided in the output log files. In Table 2, the time of a single step for each part of the computation is reported. Atomistic simulations perform complex calculation and provides detailed information which could be useful to study chemical and physical properties of the molecular system. In particular, a long simulation time is used to calculate the density matrix in SCF loop (SCF), while the time required to calculate new transmission spectrum from new density matrix ($T(\mathcal{E})$) is very small with respect to density matrix. However, such detailed information is not required by circuit simulator for electronic systems. In the proposed model EE-BESD (BL+EP+SCF-DL), we avoid recalculating the density matrix at each step and we estimate the transmission spectrum following the methodology discussed in Section 3. Thus, the simulation time is reduced of six orders of magnitude, as shown in Table 2 while maintaining the accuracy. The same is for the other two methods (BL+SCF-DL and BL+SCF-DOS). In particular, in BL+SCF-DOS the values related to $T(\mathcal{E})$ are always zero, because the BL+SCF-DOS method does not compute a new transmission spectrum after SCF loop but it is based on density of states [36,38]. In addition, the timing analysis of the BL+SCF-DOS method reveals that simulation time is higher than the proposed model (about 30% more with respect to BL+EP+SCF-DL) while the accuracy in computing I-V characteristics is reduced, as shown in figure 5. Moreover, the comparison between BL+EP+SCF-DL and BL+SCF-DL shows that the evaluation of peak improves the accuracy (see Fig. 5) and is also computationally efficient, since the increase of SCF time due to EP is less than 10%. Thus, the proposed model (BL+EP+SCF-DL) is a good compromise between computational costs and accuracy and this makes the application of our model feasible for circuit level simulations, in which a large number of devices are involved when realistic structures are considered.

Table 2 Timing analysis of different models for the calculation of current in molecular FET. For all the methods, three main contributions are considered: the self-consistent field loop (SCF), the transmission spectrum calculation ($T(\mathcal{E})$) and the calculation of current (I). Each value refers to a single step of a specific part of the method.

Molecule	BL+EP+SCF-DL (proposed) Timing (ms/step)			BL+SCF-DL Timing (ms/step)			BL+SCF-DOS Timing (ms/step)			NEGF+DFT Timing (sec/step)		
	SCF	$T(\mathcal{E})$	I	SCF	$T(\mathcal{E})$	I	SCF	$T(\mathcal{E})$	I	SCF	$T(\mathcal{E})$	I
OPV	0.79	0.19	1.34	0.78	0.20	1.28	22.4	0	22.7	2167.7	258.5	2891.2
OPE	0.99	0.20	1.49	0.98	0.20	1.43	33.9	0	34.2	2102.3	265.5	2743.0
3TT	0.75	0.25	1.36	0.71	0.21	1.18	33.2	0	33.5	1709.3	256.6	2206.5
4TT	1.10	0.22	1.73	1.10	0.22	1.62	31.7	0	32.0	1844.5	264.5	2373.3
5TT	0.91	0.19	1.46	0.91	0.20	1.38	27.8	0	28.1	2128.6	263.1	2802.9

4) Application for circuit-level simulations

The VHDL-AMS is a standard that enables the design of analog and mixed signal systems and integrated circuits [50]. Thanks to its features it is possible to implement models that encapsulate high-level behavioral descriptions and device descriptions at the physical level. In particular, with VHDL-AMS it is possible to describe a continuous model based on physical equations. This is an advantage since it allows to describe the behavior of the device starting from some physical quantities (for example the position of the energy levels or the HOMO or LUMO type conduction) and to consequently evaluate their impact on the circuit. VHDL has been invented to concurrently simulate thousands or even millions of transistors, but it is possible only if the embedded device model is computational efficient. The proposed model is a good candidate to be implemented in VHDL-AMS, due to its low computational cost and good accuracy. The modularity of the model has been reproduced in the same way in the VHDL-AMS implementation, defining different functions for each part of the model: evolution of peaks, self-consistent field loop, shifting of transmission spectrum and calculation of current. Moreover, the iterative SCF loop is kept inside the VHDL-AMS description and both the balance between accuracy and simulation time could be trimmed on demand setting the convergence parameter inside the model.

Our aim is to show that the proposed model works well at the circuit level description and can be used for circuit simulations with a high number of devices. For this reason, we focused on our previous work [51,52]: we implemented low complexity circuits (inverter, half-adder, full-adder) with a crossbar architecture in which the single device was implemented by a N-type molFET and a pull-up resistor. In this work, we implemented a structure with an increasing number of gates (from 1 to 64) connected in parallel, exploiting the proposed model as molFET description. In figure 13 the computational cost as function of the number of gates in the circuit is reported: the computational time for simulating the
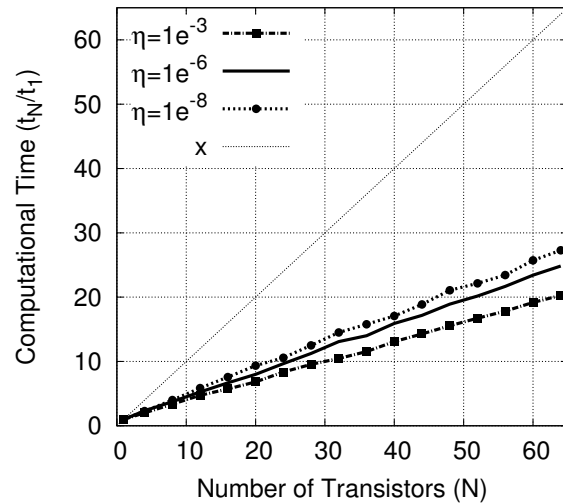

Fig. 13 CPU time as function of the increasing number of transistors for the VHDL-AMS simulation including EE-BESD as transistor model.

circuit with a generic number N of transistors (t_N) is computed and normalized with respect to the case of one single transistor (t_1). In figure 13, the results with three different values of convergence factor η for the desired accuracy (see equation (7) in Section 3(C)) are reported, as well as the bisector x for sake of linearity comparison. For all the three cases, the CPU time increases linearly with the transistor number, but, since the slope is always smaller than the bisector, the derivative is always lower than 1. In particular, the slope of the curve for $\eta = 10^{-6}$ is 0.4 and the computational time (t_N/t_1) of a system with a million of transistors is expected to be $4 \cdot 10^5$. This demonstrates that the proposed model and the overhead due to VHDL-AMS are compatible with the description of a real high complexity circuit. Finally, the results obtained show that the proposed methodology is a good approach to face with complexity level typical of high performance molecular systems, exploiting at the same time highly accurate models.

5 Conclusions

We presented a model to estimate the electron transport in molecular FET with applied bias and gate voltages. The proposed model relies on the results obtained by atomistic simulation of the molecular system under analysis without any bias conditions (e.g. at the equilibrium). In particular, given the transmission spectrum at the equilibrium and other important parameters extracted from atomistic simulations or curve fitting, the proposed model allows to compute the electron transport within the molecule for different bias voltages by means of SCF loop. Moreover, the proposed model takes also into account the effect of the gate voltage. Then, the $I - V$ characteristics of the molecular transistor can be drawn and the results obtained for the molecules analyzed in this work (OPV, OPE, 3TT, 4TT, 5TT) are comparable to atomistic simulation results, while the required CPU time is remarkably reduced. Thus, the main contributions of this work are twofold: providing an accurate model for molecular transistor and reducing the computational effort in a circuit application perspective. Finally, the applicability of the proposed model to a circuit level description is validated simulating a real circuit with an increasing number of interconnected transistors.

References

1. R. Tsui. Molecular-scale engineering for future electronics. In *Circuits and Systems, 2002. ISCAS 2002. IEEE International Symposium on*, volume 2, pages II–41. IEEE, 2002.
2. A. Pulimeno, M. Graziano, D. Demarchi, and G. Piccinini. Towards a molecular qca wire: simulation of write-in and read-out systems. *Solid State Electronics*, 77:101–107, 2012.
3. Seth Copen Goldstein and Mihai Budiu. *Molecules, Gates, Circuits, Computers*, chapter in Molecular Nanoelectronics, pages 327–388. American Scientific Publishers, January 2003.
4. A. Pulimeno, M. Graziano, and G. Piccinini. Molecule Interaction for QCA Computation. *IEEE International Conference on Nanotechnology*, pages 1–5, 2012.
5. M. Haselman and S. Hauck. The future of integrated circuits: A survey of nanoelectronics. *Proceedings of the IEEE*, 98(1):11–38, 2010.
6. M. Awais, M. Vacca, M. Graziano, and G. Masera. Quantum dot Cellular Automata Check Node Implementation for LDPC Decoders. *IEEE Transaction on Nanotechnology*, 12(3):368–377, 2013.
7. M.R. Stan, P.D. Franzon, S.C. Goldstein, J.C. Lach, and M.M. Ziegler. Molecular electronics: From devices and interconnect to circuits and architecture. *Proceedings of the IEEE*, 91(11):1940–1957, 2003.
8. C. Condo, M. Martina, and G. Masera. Vlsi implementation of a multi-mode turbo/ldpc decoder architecture. *IEEE Transactions on Circuits and Systems I: Regular Papers*, 60(6):1441–1454, 2013. cited By 10.

9. Ci Lei, D. Pamunuwa, S. Bailey, and C. Lambert. Design of robust molecular electronic circuits. In *Circuits and Systems, 2009. ISCAS 2009. IEEE International Symposium on*, pages 1819–1822, 2009.
10. Azzurra Pulimeno, Mariagrazia Graziano, and Gianluca Piccinini. Udsm trends comparison: From technology roadmap to ultrasparc niagara2. *Very Large Scale Integration (VLSI) Systems, IEEE Transactions on*, 20(7):1341–1346, 2012.
11. Mario Roberto Casu, Mariagrazia Graziano, Guido Masera, Gianluca Piccinini, and Maurizio Zamboni. An electromigration and thermal model of power wires for a priori high-level reliability prediction. *IEEE Transaction on Very Large Scale Integration (VLSI) Systems*, 12:349–358, 2004.
12. I. Rattalino, P. Motto, G. Piccinini, and D. Demarchi. A new validation method for modeling nanogap fabrication by electromigration, based on the resistance-voltage (r-v) curve analysis. *Physics Letters, Section A: General, Atomic and Solid State Physics*, 376(30-31):2134–2140, 2012. cited By 6.
13. S. Frache, D. Chiabrando, M. Graziano, M. Vacca, L. Boarino, and M. Zamboni. Enabling design and simulation of massive parallel nanoarchitectures. *Journal of Parallel and Distributed Computing*, 74(6):2530–2541, 2014. cited By 3.
14. Roald Hoffmann. An Extended Hückel Theory. I. Hydrocarbons. *The Journal of Chemical Physics*, 39:1397, 1963.
15. Daniel SanchezPortal, Pablo Ordejon, Emilio Artacho, and Jose M. Soler. Density-functional method for very large systems with LCAO basis sets. *International Journal of Quantum Chemistry*, 65(5):453–461, 1997.
16. Mads Brandbyge, José-Luis Mozos, Pablo Ordejón, Jeremy Taylor, and Kurt Stokbro. Density-functional method for nonequilibrium electron transport. *Physical Review B*, 65(16):165401, 2002.
17. Supriyo Datta. The non-equilibrium Green's function (NEGF) formalism: An elementary introduction. In *Electron Devices Meeting, 2002. IEDM'02. International*, pages 703–706. IEEE, 2002.
18. P.A. Derosa and M. Jorge. Electron transport through single molecules: Scattering treatment using density functional and Green function theories. *The Journal of Physical Chemistry B*, 105(2):471–481, 2001.
19. A. Aviram and M.A. Ratner. Molecular rectifiers. *Chemical Physics Letters*, 29(2):277–283, 1974.
20. M. Di Ventra, ND Lang, and ST Pantelides. Electronic transport in single molecules. *Chemical physics*, 281(2):189–198, 2002.
21. H. Song, M.A. Reed, and T. Lee. Single molecule electronic devices. *Advanced Materials*, 23(14):1583–1608, 2011.
22. X. Chen, A.B. Braunschweig, M.J. Wiester, S. Yeganeh, M.A. Ratner, and C.A. Mirkin. Spectroscopic tracking of molecular transport junctions generated by using click chemistry. *Angewandte Chemie International Edition*, 48(28):5178–5181, 2009.
23. H. Song, Y. Kim, H. Jeong, M.A. Reed, and T. Lee. Coherent tunneling transport in molecular junctions. *J. Phys. Chem. C*, 114:20431–20435, 2010.
24. R. Yamada, H. Kumazawa, T. Noutoshi, S. Tanaka, and H. Tada. Electrical conductance of oligothiophene molecular wires. *Nano letters*, 8(4):1237–1240, 2008.
25. R. Yamada, H. Kumazawa, S. Tanaka, and H. Tada. Electrical resistance of long oligothiophene molecules. *Applied physics express*, 2(2):5002, 2009.

26. L.A. Zotti, T. Kirchner, J.C. Cuevas, F. Pauly, T. Huhn, E. Scheer, and A. Erbe. Revealing the role of anchoring groups in the electrical conduction through single-molecule junctions. *Small*, 6(14):1529–1535, 2010.

27. Jeong-O Lee, Gnther Lientschnig, Frank Wiertz, Martin Struijk, Rne A. J. Janssen, Richard Egberink, David N. Reinhoudt, Peter Hadley, and Cees Dekker. Absence of strong gate effects in electrical measurements on phenylene-based conjugated molecules. *Nano Letters*, 3(2):113–117, 2003.

28. H. Song, Y. Kim, Y.H. Jang, H. Jeong, M.A. Reed, and T. Lee. Observation of molecular orbital gating. *Nature*, 462(7276):1039–1043, 2009.

29. S.S. Datta, D.R. Strachan, and A.T.C. Johnson. Gate coupling to nanoscale electronics. *Physical Review B*, 79(20):205404, 2009.

30. Kai Xiao, Yunqi Liu, Ting Qi, Wei Zhang, Fang Wang, Jianhua Gao, Wenfeng Qiu, Yongqiang Ma, Guanglei Cui, Shiyan Chen, Xiaowei Zhan, Gui Yu, Jingui Qin, Wenping Hu, and Daoben Zhu. A highly -stacked organic semiconductor for field-effect transistors based on linearly condensed pentathienoacene. *Journal of the American Chemical Society*, 127(38):13281–13286, 2005. PMID: 16173758.

31. Minliang Zhu, Hao Luo, Liping Wang, Yunlong Guo, Weifeng Zhang, Yunqi Liu, and Gui Yu. The synthesis of 2,6-dialkylphenyldithieno[3,2-b:2,3-d]thiophene derivatives and their applications in organic field-effect transistors. *Dyes and Pigments*, 98(1):17 – 24, 2013.

32. Ahmed Mahmoud and Paolo Lugli. First-principles study of a novel molecular rectifier. 2013.

33. G. Feng, N. Wijesekera, and T.L. Beck. Real-space multigrid method for linear-response quantum transport in molecular electronic devices. *Nanotechnology, IEEE Transactions on*, 6(2):238–244, 2007.

34. P. Bai, E. Li, P. Collier, et al. Theoretical investigation of metal-molecule interface with terminal groups. *Nanotechnology, IEEE Transactions on*, 4(4):422–429, 2005.

35. J. Fransson, O.M. Bengone, J.A. Larsson, and J.C. Greer. A physical compact model for electron transport across single molecules. *Nanotechnology, IEEE Transactions on*, 5(6):745–749, 2006.

36. S. Datta. *Quantum Transport: Atom to Transistor.* . Cambridge University Press, 2005.

37. Ferdows Zahid, Magnus Paulsson, and Supriyo Datta. Electrical conduction through molecules. *Advanced Semiconductors and Organic Nano-Techniques*, 2003.

38. S. Datta. *Electronic transport in mesoscopic systems*. Cambridge university press, 1997.

39. D. Hou and J. H. Wei. The difficulty of gate control in molecular transistors. *ArXiv e-prints*, September 2011.

40. C.C. Kaun and T. Seideman. The gating efficiency of single-molecule transistors. *Journal of Computational and Theoretical Nanoscience*, 3(6):951–956, 2006.

41. Ahmed Mahmoud and Paolo Lugli. Transport characterization of a gated molecular device with negative differential resistance. In *Nanotechnology (IEEE-NANO), 2012 12th IEEE Conference on*, pages 1–5. IEEE, 2012.

42. Yuqing Xu, Changfeng Fang, Bin Cui, Guomin Ji, Yaxin Zhai, and Desheng Liu. Gated electronic currents modulation and designs of logic gates with single molecular field effect transistors. *Applied Physics Letters*, 99(4):043304–043304, 2011.

43. Santanu K Maiti. Multi-terminal quantum transport through a single benzene molecule: Evidence of a molecular transistor. *Solid State Communications*, 150(29):1269–1274, 2010.

44. Ahmed Mahmoud and Paolo Lugli. Towards circuit modeling of molecular devices. 2014.

45. Atomistix ToolKit version 12.8 quantumwise a/s.

46. Mads Brandbyge, José-Luis Mozos, Pablo Ordejón, Jeremy Taylor, and Kurt Stokbro. Density-functional method for nonequilibrium electron transport. *Phys. Rev. B*, 65:165401, Mar 2002.

47. Hans Henrik B. Sørensen, Per Christian Hansen, Dan Erik Petersen, Stig Skelboe, and Kurt Stokbro. Krylov subspace method for evaluating the self-energy matrices in electron transport calculations. *Phys. Rev. B*, 77:155301, Apr 2008.

48. José M Soler, Emilio Artacho, Julian D Gale, Alberto García, Javier Junquera, Pablo Ordejón, and Daniel Sánchez-Portal. The siesta method for ab initio order-n materials simulation. *Journal of Physics: Condensed Matter*, 14(11):2745, 2002.

49. Y. Ai and H-L. Zhang. Construction and conductance measurement of single molecule junctions. *Acta Phys. -Chim. Sin.*, 28(10):2237–2248., 2012.

50. Vhdl analog and mixed-signal extensions, 1999. IEEE Std. 1076.1.

51. A. Zahir, S.A.A. Zaidi, A. Pulimeno, M. Graziano, D. Demarchi, G. Masera, and G. Piccinini. Molecular transistor circuits: From device model to circuit simulation. In *Nanoscale Architectures (NANOARCH), 2014 IEEE/ACM International Symposium on*, pages 129–134, July 2014.

52. A. Zahir, A. Mahmoud, A. Pulimeno, M. Graziano, G. Piccinini, and P. Lugli. Hierarchical modeling of opv-based crossbar architectures. In *Nanotechnology (IEEE-NANO), 2014 14th IEEE Conference on*, pages 1–5. IEEE, 2014.